Proceedings of the 8th World Congress on Mechanical, Chemical, and Material Engineering (MCM'22)
Prague, Czech Republic – July 31, 2022 - August 02, 2022
Paper No. HTFF 165
DOI: 10.11159/htff22.165

Development of a Thermal Mass Airflow Sensor for Low-Velocity Ducted Flow Applications

Eoin Guinan[1], Conor Macken[3], Vanessa Egan[2]
[1]CONNECT, Stokes Laboratories, Bernal Institute, University of Limerick, Ireland, V94 T9PX
[2]School of Engineering, University of Limerick, Ireland, V94 T9PX
[3]Galway Technology Park, Parkmore, Galway Ireland
Eoin.Guinan@ul.ie
Conor.Macken@woodplc.com
Vanessa.Egan@ul.ie

Abstract **-** This study was conducted to develop a flat plate, calorimetric based, mass airflow sensor capable of measuring low-speed flow typically found in heating, ventilation, and air conditioning (HVAC) systems. Moreover, to develop a numerical model that accurately predicts the fluidic and thermal behaviour of the sensor design. Current findings indicate that the numerical and experimental results were in close agreement, with the predicted leading-edge temperatures within 1-2% of those recorded experimentally. However, this error increased in the trailing edge to a maximum of 8%; inclusion of the trailing edge flap within the numerical model reduced this to less than 3%, suggesting that the flap generates enhanced cooling within the trailing region. The temperature deltas predicted by the numerical model were on average twice that of the experimental values, however, the average temperature change was still less than 0.03°C per 1 m/s increase in velocity. It was concluded that the copper sensor design was unsuitable for mass flow measurement. The numerical findings for the stainless-steel sensor indicate a 600% increase in the maximum temperature delta measured from 0.069°C to 0.49°C. Which suggests the subsequent increase in accuracy is a result of the decreased thermal diffusivity of stainless-steel, which is 96% lower than that of copper. Other findings include, a further increase in temperature delta values when the heater size is decreased, resulting in a maximum temperature delta value of 0.58°C and an average change of 0.49°C for a 1 m/s change in flow velocity. Thus, it can be implied that the modified calorimetric airflow sensor would accurately predict the mass flow rates within HVAC ducting systems.

Keywords**:** Thermal flow meter, Flat plate, Calorimetric principle, Low velocity flow, HVAC systems

1. Introduction

Current statistics on energy consumption report that buildings account for 40% of the global primary energy requirements [1]. A large contributor to this energy requirement is heating, ventilation and air conditioning (HVAC) systems. These systems consume large amounts of electricity due to the energy required to heat and cool a room through radiators, heated air ducting, underfloor heating or air conditioning units. This trend of high energy consumption will most likely continue, as thermal comfort is ranked highest among building requirements ahead of indoor air quality and acoustic comfort [2]. Much of the current research on HVAC systems is focused on efficiency [3-4], with energy savings of 30% possible by utilising Energy Management Systems (EMS) [4]. A parameter critical to the implementation and optimisation of HVAC systems through EMS is the mass flow of air (inflow and outflow); as air is the primary medium of thermal transport, therefore, the respective flow rates can be used to quantify the amount of heat addition and heat loss occurring [3]. Mass flow sensors are devices that determine the rate of mass transfer inside conduits or ducts through correlation with physical and thermal phenomenon. These sensors are significantly more accurate than volumetric based sensors as they eliminate inaccuracies resulting from changes in fluidic properties as mass is not temperature and pressure dependant. Mass flow sensors operating through thermal principles are of particular interest in HVAC applications [5] as they provide highly accurate measurements at low flow rates (like those found within HVAC ducting), are capable of wide linear measurement ranges, yield minimal flow restriction, and have an absence of moving parts [6].

Thermal mass flow sensors are primarily used in gas and air flow rate measurement applications. They operate based on the principle of directing a flowing fluid, such as air, over a heater and measuring its effect on the heater, or conversely, the heaters effect on it. The three most common types are thermal dispersion, thermal pulse, and calorimetric. Thermal dispersion

sensors utilise Newton's law of cooling to determine mass flow rate by means of quantifying the thermal energy dissipated by convection from a heated element to a surrounding fluid [6]. Generally, the heated element consists of a cylindrical wire or a flat film, through which a current is passed. The effects of fluid flow are evaluated differently depending on the operational mode of the sensor. Measuring the heating power or heater temperature and relating this to the current flow results in two possible operational modes; a constant temperature (CT) mode ($\Delta Q \sim \dot{m}$) and a constant power (CP) mode ($T^{-1} \sim \dot{m}$). Thermal pulse sensors operate by measuring the transit time of a pulse of heat introduced into a flowing liquid, which subsequently, carries it a specified distance to a downstream temperature sensor. The lower the flow velocity is, the longer it takes for the pulse to travel to the downstream temperature sensing element. The transit time is therefore directly related to the flow velocity ($t_{transit} \sim \dot{m}$). Calorimetric flow meters operate based on the generation of an asymmetrical temperature distribution around a centrally located heater as a result of fluid flow, or, more specifically boundary layer development. Pairs of temperature sensing elements are located upstream and downstream of the heater allowing for constant monitoring of the temperature distribution. In a case of zero flow, the temperature distribution is symmetrical with respect to the heater, thus the temperature difference between them is equal to zero. The velocity of the measured flow is proportional to the magnitude of the temperature delta between respective temperature sensor pairs ($\Delta T \sim \dot{m}$).

Recently the suitability of calorimetric flow sensors was highlighted for use in HVAC systems by utilising printed board technology [5]; the sensors developed were designed to be robust, cost-effective, and suitable for mass production. However, it was found that the maximum measurable flow velocity was only 0.5 m/s beyond which signal saturation occurred, as such, they did not meet the requirements for implementation into HVAC systems where velocities can reach up to 10 m/s. Most of the current literature on the development of calorimetric sensors for low-velocity flow has focused on milli and micro scale (10 mm to 10 μm), however, it has been indicated that sensors of this size have a limited measurement range due to the globalised cooling effect experienced at higher flow rates [7], Although, existing studies have illustrated the feasibility of calorimetric flow sensors for the measurement of low-speed flows [5], the implementation of a larger scale sensor cable of measuring flow rates consistent with that found in HVAC systems (1-10 m/s) has yet to be presented in the literature. Hence, this study details the design, calibration, and testing of an experimental calorimetric flow sensor intended for use in HVAC systems. Additionally, modern numerical techniques are employed to gain deeper insight into the fluidic and thermal phenomena occurring during operation. The data gathered from the numerical model is compared to that of the experimental results to assess its validity. Subsequently, the numerical model is further developed over a range of flow rates, heat inputs, material properties, and temperature sensor locations to assess their effect on the overall performance and reliability of the flow sensor.

2. Experimentation

2.1 Wind Tunnel

As previously discussed, calorimetric sensors detect flow by monitoring the generation of an asymmetrical temperature distribution around a centrally located heater as a result of fluid flow. As the flow velocity increases the magnitude of the temperature delta decreases. This decrease is proportional to the increase in velocity and by extension the mass flow rate if the velocity profile and duct geometry are known. To function, the sensor must be 'mapped' to relate known velocity values to the measured temperature difference. Mapping was carried out using a low-speed open circuit suction wind tunnel that operates using four parallel fans. It has two honeycomb panels and a settling chamber to ensure laminar flow. The dimensions of the tests section are reflective of a HVAC duct cross-section, 30 x 30 mm. The velocity profile within the wind tunnel was characterised using a static Pitot tube to ensure the flow was uniform and laminar across the cross-section of the test section. The control voltage supplied to the fans was varied from 1 V to 2 V in increments of 0.1V for a total of eleven data points. The velocity profiles obtained for each voltage are detailed in Fig.1(a) below.

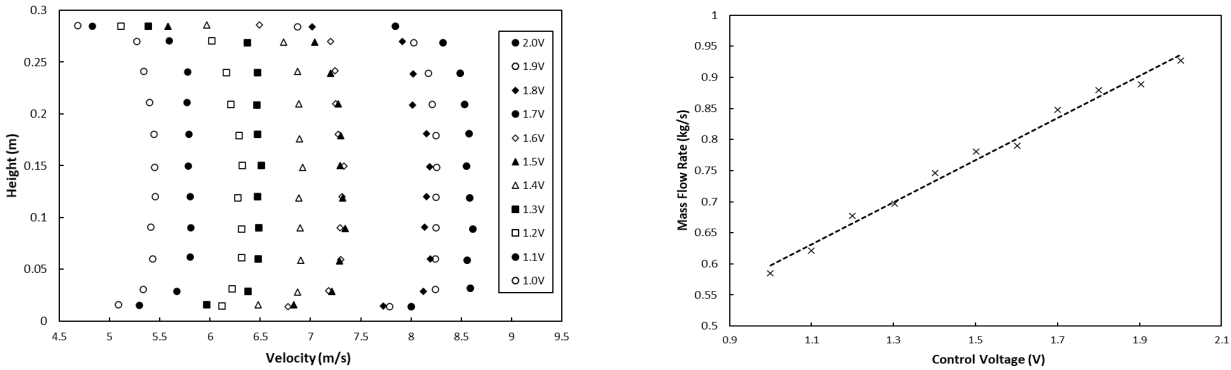

Fig.1: The velocity profiles within the wind tunnel for control voltages 1-2V (a)(left) and corresponding mass flow rates (b)(right). (b)(right).

2.2 Calorimetric Sensor

The calorimetric sensor design, as illustrated in Fig.2, consists of a flat copper plate of streamwise length 240 mm with a centrally located 100 x 100 mm 10W Rs Pro silicone resistive heater mat (PN: 245-540). To ensure proper attachment of the hydrodynamic boundary layer and to prevent premature downstream flow separation the design incorporates a super ellipse leading-edge shape and trailing edge flap. Separation often occurs due to a rapid increase in pressure between the leading edge and flat plate geometry [8]. This rapid increase is described by the pressure coefficient of the flow, a dimensionless number used to determine if an inverse pressure gradient is developing along the leading edge. The aspect ratio of the leading edge has been shown to minimise the pressure coefficient [9], with aspect ratios greater than five shown to minimise separation [10], as such an aspect ratio of six was used in this design. Similarly, the trailing edge flap is utilised to prevent flow separation by controlling the stagnation point of the flow and ensuring it occurs at the tip of the leading edge. Geometrically, the flap is similar to those used in other studies [9], with a length of 36 mm (15% of the total plate length). It was found that an angle of 45° to the flow direction was most effective in minimising premature boundary layer separation.

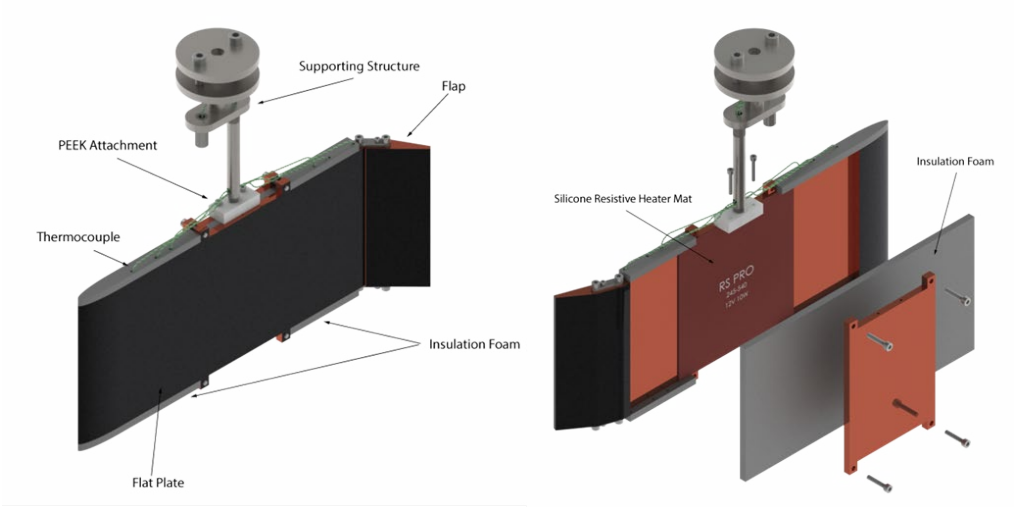

Fig.2: Calorimetric flow sensor design and experimental setup.

The temperature distribution was measured by seven RS Pro K-type thermocouples (accuracy of ±0.1°C) inserted into corresponding 50 mm deep, 1 mm diameter holes located symmetrically around the silicone resistive heater mat. These holes were drilled at distances of 10 mm, 22.5 mm, and 42.5 mm from the edge of the heated section as displayed in Fig.3.

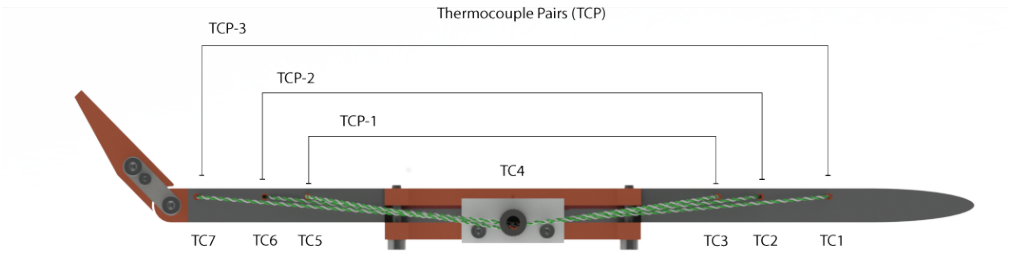

Fig.3: Thermocouple layout and trailing edge flap.

An additional thermocouple was used to measure ambient temperature during each test. Dow corning 340 heat sink compound was applied to each of the thermocouples to reduce measurement uncertainties associated with thermal contact resistance between the thermocouples and the flat plate. The thermocouples were connected to a data acquisition system consisting of an Arduino Nano and seven AD7790 voltage amplifiers to read the output of each thermocouple. Communication code was written in MATLAB to obtain serial data from the Arduino to process the experimental results and control the power input. The Arduino uses Pulse Width Modulation (PWM) and the control circuit to adjust the power input supplied to the resistive heater mat. Power was supplied by a ZP-DP60 Step Down-Up Power Supply with a max voltage output of 29V.

To ensure correct operation of the calorimetric flow meter as an idealised flat plat in parallel flow, it is necessary to limit convective heat losses to the front face of the flat plate. To achieve this polyurethane insulation foam was applied to the edges and rear of the plate, as illustrated in Fig.2. It is also critical that radiative losses can be determined, as such, the exposed surfaces of the calorimeter were sprayed black increasing the surface emissivity close to unity. To allow for the attachment of the flow meter to wall of the wind tunnel test section a supporting structure was designed. It consists of round stainless-steel tubes which act to reduce conductive heat loss from the system by reducing the effective area for conduction. To further reduce conductive losses, a PEEK fixture, with an effective thermal conductivity of 0.25 W/mK, is used to attach the calorimetric flow sensor to the supporting structure.

As detailed in section 2.1, the sensor must be ‘mapped’ or characterised to relate the known velocity values and mass flow rates to the measured temperature difference within the flat plate. This requires knowledge of the velocity profile of the tunnel to relate the temperature difference taken at that point to the average flow velocity. These velocities were determined prior to testing and were presented in the previous section. To initialise the characterisation procedure the wind tunnel was supplied with an initial control voltage of 2 V. Subsequently, the data recorder was activated, and a 20 W power input was supplied to the restive heater mat until a quasi-steady state was reached; defined as a temperature delta of less than 0.5°C over a 15-minute period in all thermocouples. Once achieved, the temperature profile within the plate was recorded. The control voltage was then reduced in increments of 0.2 V until 1 V is reached (minimum control voltage to activate the four fans). This process was repeated for power inputs of 25 W and 30 W.

3. Numerical Analysis

Steady three-dimensional finite element numerical models were developed to predict the thermal and fluidic behaviour of the sensor during operation. Moreover, once validated by experimental data, these models were used to optimise the design and inform future experimental work. This study utilised the conjugate solver within Siemens PLC Star CCM+. Conjugate heat transfer refers to a heat transfer process that involves the interaction of both conduction within a solid and convection from the solid surface to a fluid flow [11-12]. Therefore, it is necessary to couple the equations governing conduction within the solid to those governing convection in the fluid flow and subsequently solve them simultaneously using numerical solvers. The sensor was modelled in a fluid region (air) that has the same dimensions as the wind tunnel test section, with a laminar fluid flow boundary condition applied to the inlet face resulting in air flow from left to right, see Fig.4. Flow was solved using a second order upwind scheme pressure-based solver. A

no slip condition was defined at the interface between the sensor and the fluid region to ensure accurate development of the hydrodynamic and thermal boundary layers. It was also defined at the walls of the fluid region to replicate the parabolic velocity profile identified during wind tunnel characterisation in section 2.1. Both the initial temperature of the sensor and surrounding flow was set to 15°C (experimental ambient temperature). Bulk material parameters were applied to each region of the model. To simulate the resistive heater mat attached to the underside of the copper plate, a constant heat flux condition was applied over the same area. This was varied from 20-30 W to allow for comparison to experimental data.

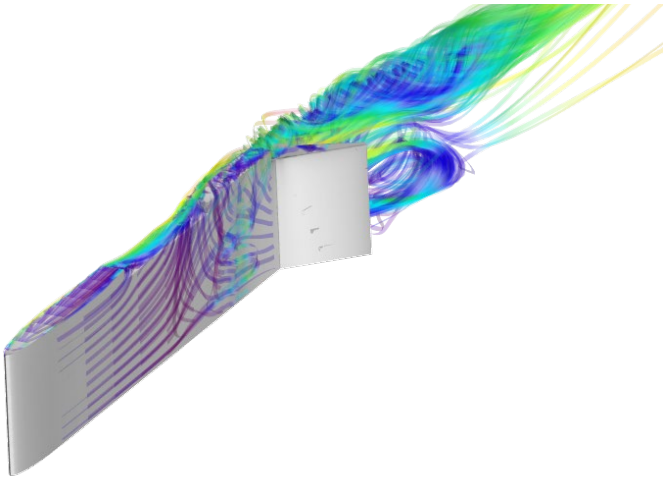

Fig.4: Copper calorimetric flow meter immersed in a 5.3 m/s air flow travelling from left to right.

4. Results & Discussion

4.1 Copper Sensor

The numerical and experimental results for a 20 W heating power input are displayed in Fig.5a-5b below. It is evident that the desired asymmetric temperature distribution is occurring with temperatures in the trailing edge, between 195-240mm, noticeably higher than those at the leading edge, between 40-75mm. However, the magnitude of the changes in temperature distribution relative to change in velocity are minimal, as indicated in Fig.5(b). Minimal changes in ΔT would present major issues during operation of the sensor, as flow velocities could not accurately be related to changes in temperature distribution. Any sensor used would require a temperature resolution of order ±0.01°C. This is an undesirable trait for a flow sensor and also raises the issue of the uncertainty of the measurement.

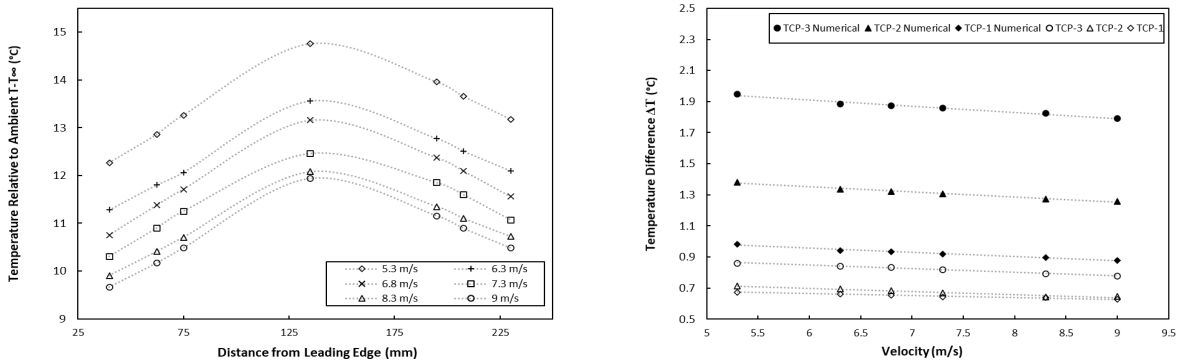

Fig.5: Numerical and experimental temperature distribution along the length of the copper plate (a) (Left) and respective temperature distribution changes relative to velocity increase (b) (Right) for a 20 W heater input.

As seen in Fig.5(b), the changes in temperature difference between respective thermocouple pairs is evidently not of a suitable magnitude for mass flow measurements. It was found that the third thermocouple pair (TCP-3) provided the most consistent changes in temperature delta with increasing velocity; a maximum of 0.03°C for a 1 m/s increase. This was expected as TCP-3 operates at a higher temperature difference due to an increased distance for boundary layer development and large temperature drop from conduction in comparison to the pairs located closer to the heater.

Comparing both the numerical and experimental results in Fig.5(b), it was observed that the magnitude of the numerical asymmetrical temperature distribution was more twice that of the experimental at a given velocity and a similar trend was observed for the numerical temperature distribution change with increase in velocity. Predicted temperatures within the trailing edge were 18-21% higher than that of experimental, indicating enhanced cooling within this region. Inclusion of the trailing edge flap in the numerical model reduced this to 1-4%. Fig.6(a)-6(b) display the pressure and temperature contour plots of the region immediately upstream of the flap, it is evident that the adverse pressure gradient generated by the flap results in premature flow separation disrupting the hydrodynamic and thermal boundary layers, see highlighted region in Fig.5(b). This disruption is detrimental to the operation of the sensor as it likely results in enhanced cooling within this region decreasing the desired temperature distribution asymmetry. It is also speculated that the high thermal diffusivity of the copper plate and subsequent high axial heat flux is equally detrimental to the operation of the sensor as it induces premature and rapid growth of the thermal boundary layer in the leading section. As previously discussed, thermal boundary layer growth and by extension hydrodynamic growth is ultimately what results in the development of an asymmetrical temperature distribution, the location and rate at which it develops can dictate the profile of temperature distribution induced.

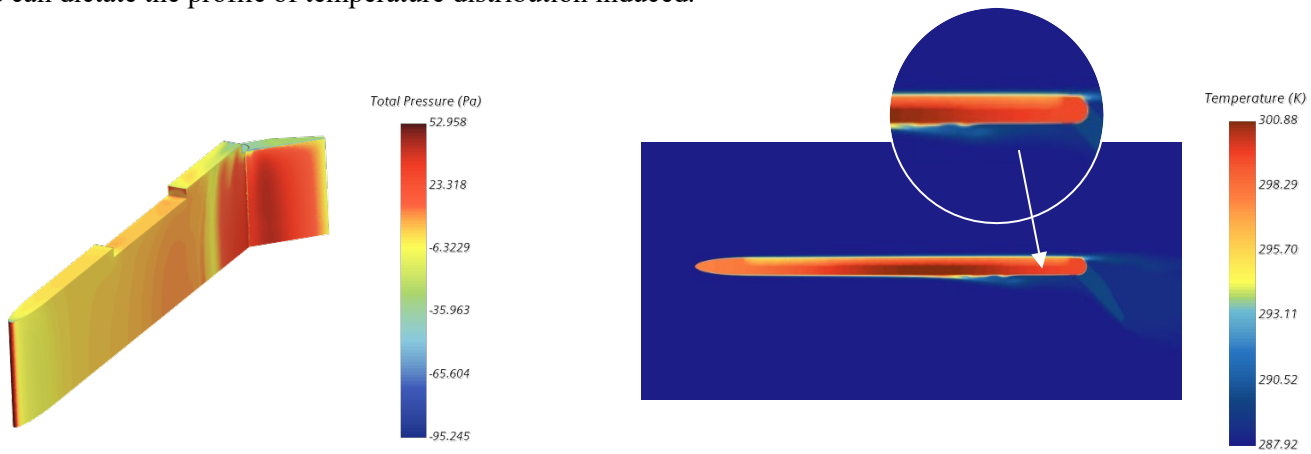

Fig.6: Pressure (a)(left) and temperature (b)(right) contour plot of copper calorimetric flow meter with the trailing edge flap modelled.

4.2 Stainless-Steel Sensor

The objective of replacing the copper plate with a stainless-steel plate is to induce a significantly steeper and more pronounced temperature distribution, yielding temperature differences that are more consistent and larger in magnitude relative to changes in airflow velocity. To assess the validity of this design change, the experimentally validated numerical model was employed. The numerical temperature distributions for a 20 W heating power input are displayed in Fig.7a. In comparison to Fig.5a the asymmetrical temperature distribution at all flow rates is significantly steeper and more pronounced. Furthermore, the magnitude of the temperature difference between the leading and trailing edge is observed to be significantly greater. The numerical model also predicts independent development of the hydrodynamic and thermal boundary layers, with the latter developing much further along the plate. This is indicative of greater changes in temperature distribution relative to change in velocity. The numerical temperature distribution changes relative to velocity are displayed in Fig.7b for all thermocouple pairs. It was observed that the temperature deltas measured by the third thermocouple pair furthest from the heater, were significantly greater in magnitude comparative to those measured

by the copper sensor. Previously, the maximum change measured was 0.07°C for a corresponding increase in velocity of 1 m/s. The stainless-steel sensor achieved a maximum change of 0.49°C for the same change in flow velocity, a 600% increase.

As previously observed, the temperature deltas measured by the thermocouple pairs located closest to the heater are minimal comparative to the third thermocouple pair, it was hypothesized that their proximity to the heater was detrimental to creating the desired changes in temperature delta relative to velocity. The results of reducing the heater size to 50 mm are a displayed in Fig.8(a)-8(b). It is evident that a much steeper temperature distribution is generated along the length of the stainless-steel plate as a consequence of the reduction in heater size. An 18% increase, 0.49°C to 0.58°C, in the maximum temperature distribution change relative to velocity was achieved. An interesting observation is that TCP-1 and TCP-2 did not experience any significant increase in performance, indicating that heater proximity has a minimal effect on the temperature delta changes induced. Moreover, suggesting that thermocouple placement relative to the leading edge and by extension hydrodynamic boundary layer development are now the limiting factor.

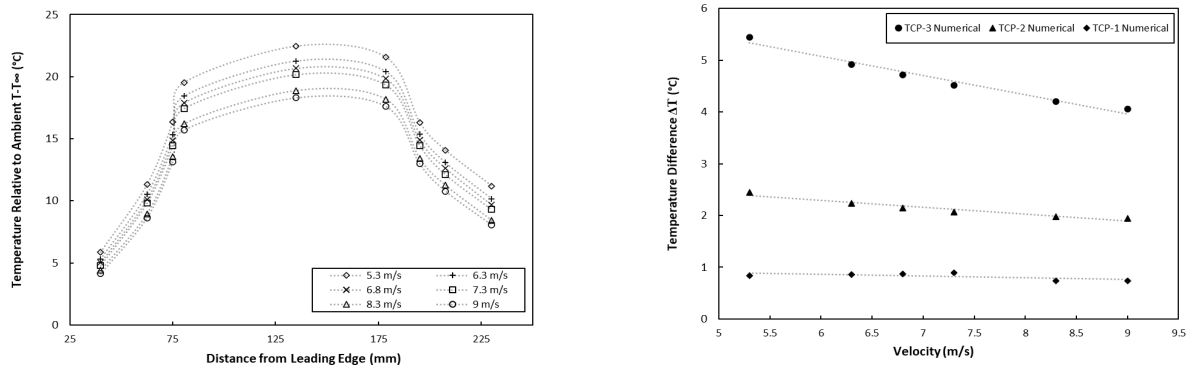

Fig.7: Numerical temperature distribution along the length of the stainless-steel plate with a 100 mm heated section (a) (Left) and temperature distribution changes relative to velocity increase (b) (Right) for a 20 W heater input.

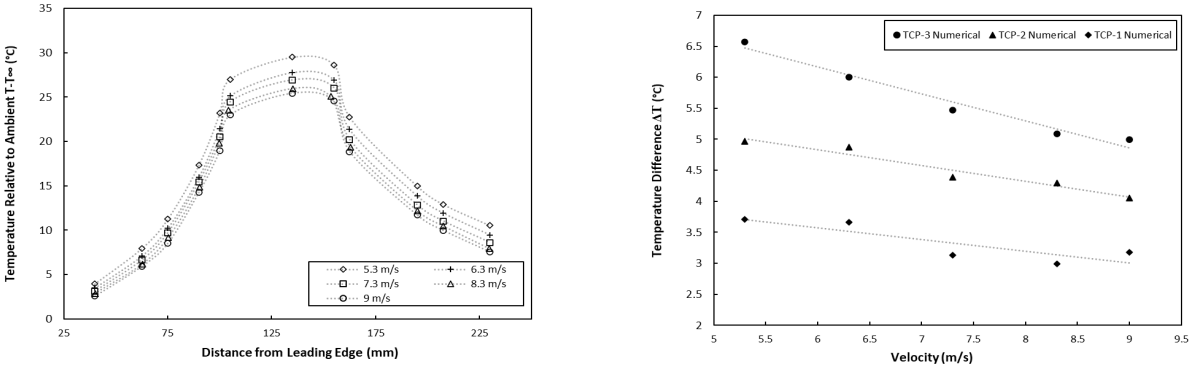

Fig.8 Numerical temperature distribution along the length of the stainless-steel plate with a 50 mm heated section (a) (Left) and temperature distribution changes relative to velocity increase (b) (Right) for a 20 W heater input

5. Conclusion

The objective of this study was to develop a mass airflow sensor capable of measuring low-speed flow typically in HVAC systems and a numerical model that accurately predicts the fluidic and thermal behaviour of the calorimetric design. It was found that the initial copper design did not achieve the necessary changes in temperature distribution to velocity required for mass flow measurement, with a maximum change of 0.07°C for a 0.8 m/s velocity increase. Close agreement was found between then numerical model and experimental results, with temperatures within the leading edge being predicted within ±2% of those experimentally measured; however, a trend of increased error was observed in the trailing edge. The lower trailing edge temperatures from the experimental model suggest that there is enhanced cooling occurring within this region. It was observed that the inclusion of the trailing edge flap adversely effected the development of the upstream boundary layer, resulting significantly reduced the trailing edge temperatures in the numerical model. Consequently, it was determined that the trailing edge flap is detrimental to the operation of the calorimetric flow meter due to its adverse effects on the development of the desired asymmetric temperature distribution.

The numerical model was then further developed, by replacing the copper plate with a stainless-steel plate. The change resulted in a significantly steeper and more pronounced temperature distribution, yielding much larger temperature deltas. The maximum change measured increased from 0.07°C for a corresponding increase in velocity of 0.8m/s to 0.49°C for the same change in velocity. This decreases the required resolution and accuracy of the thermocouples from ±0.01°C to ±0.1°C. Overall results indicate that the stainless-steel flow meter is capable of measuring the mass flow rates experienced within HVAC systems to a relatively high degree of accuracy. Consequently, it can be concluded that the low thermal conductivity of stainless-steel is of a significant benefit to the operation of the calorimetric flow meter. It was also observed that further modifications, such as a decreased heater size resulted in larger and more consistent temperature deltas, yielding a maximum temperature change of 0.57°C for a corresponding increase in velocity of 1 m/s, with an average change of 0.49°C. This suggests that the accuracy of the calorimetric flow meter would be further increased through the implementation of these modifications.

References

[1] W. Shi, X. Jin, and Y. Wang, "Evaluation of energy saving potential of HVAC system by operation data with uncertainties," *Energy and Buildings*, vol. 204, p. 109513, Dec. 2019, doi: 10.1016/J.ENBUILD.2019.109513.

[2] M. Frontczak and P. Wargocki, "Literature survey on how different factors influence human comfort in indoor environments," *Building and Environment*, vol. 46, no. 4, pp. 922–937, Apr. 2011, doi: 10.1016/J.BUILDENV.2010.10.021.

[3] L. Pérez-Lombard, J. Ortiz, I. R. Maestre, and J. F. Coronel, "Constructing HVAC energy efficiency indicators," *Energy and Buildings*, vol. 47, pp. 619–629, Apr. 2012, doi: 10.1016/J.ENBUILD.2011.12.039.

[4] R. Z. Homod, "Analysis and optimization of HVAC control systems based on energy and performance considerations for smart buildings," *Renewable Energy*, vol. 126, pp. 49–64, Oct. 2018, doi: 10.1016/J.RENENE.2018.03.022.

[5] T. Glatzl, H. Steiner, F. Kohl, F. Keplinger, and T. Sauter, "Thermal Flow Sensor based on Printed Circuit Board Technology for Ventilation and Air Conditioning Systems," *Procedia Engineering*, vol. 87, pp. 1342–1345, Jan. 2014, doi: 10.1016/J.PROENG.2014.11.711.

[6] A. Bekraoui and A. Hadjadj, "Thermal flow sensor used for thermal mass flowmeter," *Microelectronics Journal*, vol. 103, p. 104871, Sep. 2020, doi: 10.1016/J.MEJO.2020.104871.

[7] Y. Valizadeh Yaghmourali, N. Ahmadi, and E. Abbaspour-sani, "A thermal-calorimetric gas flow meter with improved isolating feature," *Microsystem Technologies*, vol. 23, Jun. 2017, doi: 10.1007/s00542-016-2915-2.

[8] R. Narasimha and S. N. Prasad, "Leading edge shape for flat plate boundary layer studies," *Experiments in Fluids*, vol. 17, no. 5, pp. 358–360, 1994, doi: 10.1007/BF01874418.

[9] R. E. Hanson, H. P. Buckley, and P. Lavoie, "Aerodynamic optimization of the flat-plate leading edge for experimental studies of laminar and transitional boundary layers," *Experiments in Fluids*, vol. 53, no. 4, pp. 863–871, 2012, doi: 10.1007/s00348-012-1324-2.

[10] E. J. Davis and W. N. Gill, "The effects of axial conduction in the wall on heat transfer with laminar flow," *International Journal of Heat and Mass Transfer*, vol. 13, no. 3, pp. 459–470, Mar. 1970, doi: 10.1016/0017-9310(70)90143-2.

[11] T. L. Perelman, "ON CONJUGATED PROBLEMS OF HEAT TRANSFER," *International Journal of Heat and Mass Transfer*, vol. 3, pp. 293–303, 1961.

[12] K. D. Cole, "Conjugate heat transfer from a small, heated strip," *International Journal of Heat and Mass Transfer*, vol. 40, no. 11, pp. 2709–2719, Jul. 1997, doi: 10.1016/S0017-9310(96)00232-3.